

# Magnetic order in lightly doped $\text{La}_{2-x}\text{Sr}_x\text{CuO}_4$

A. Gozar<sup>1,2,\*</sup>, B.S. Dennis<sup>1</sup>, and G. Blumberg<sup>1†</sup>

<sup>1</sup>*Bell Laboratories, Lucent Technologies, Murray Hill, NJ 07974*

<sup>2</sup>*University of Illinois at Urbana-Champaign, IL 61801-3080*

Seiki Komiya and Yoichi Ando

*Central Research Institute of Electric Power Industry, Komae, Tokyo 201-8511, Japan*

(Dated: February 2, 2008)

We study long wavelength magnetic excitations in lightly doped  $\text{La}_{2-x}\text{Sr}_x\text{CuO}_4$  ( $x \leq 0.03$ ) detwinned crystals. The lowest energy magnetic anisotropy induced gap can be understood in terms of the antisymmetric spin interaction inside the antiferromagnetic (AF) phase. The second magnetic resonance, analyzed in terms of in-plane spin anisotropy, shows unconventional behavior within the AF state and led to the discovery of collective spin excitations pertaining to a field induced magnetically ordered state. This state persists in a 9 T field to more than 100 K above the Néel temperature in  $x = 0.01$ .

PACS numbers: 78.30.Am, 74.72Dn, 75.30.Gw, 75.50.Ee

At short wavelengths the spin excitations in underdoped 2D cuprates are governed by the large antiferromagnetic (AF) superexchange,  $J \approx 145$  meV, while in the long wavelength limit the magnetic energy scales are set by small anisotropy parameters [1, 2, 3]. In spite of the relative weakness, the impact of the low energy magnetism on the carrier and lattice dynamics in detwinned  $\text{La}_{2-x}\text{Sr}_x\text{CuO}_4$  crystals has been shown recently to be unexpectedly large. Magnetic susceptibility data show a persistent spin anisotropy even outside the AF region [4] while the transport properties revealed besides a sizeable anisotropy of the in-plane dc resistivity [5] also a large low temperature magnetoresistance [6]. These effects call for an investigation of long wavelength magnetic excitations using a high resolution probe. A magnetic field study is of particular interest because of the surprising discovery in  $x = 0.01$   $\text{La}_{2-x}\text{Sr}_x\text{CuO}_4$  at room temperature of magnetic field induced structural changes [7], phenomenon which makes this compound unique because of the existence of strong AF correlations.

Underdoped  $\text{La}_{2-x}\text{Sr}_x\text{CuO}_4$  crystals are slightly orthorhombic below 300 K and long range AF order exists for  $x \leq 0.02$ . The layered structure allows for a XY spin anisotropy which in the spin-wave approximation leads to an out-of-plane polarized gap,  $\Delta_{XY}$  [8]. The in-plane orthorhombicity and the spin-orbit coupling lead to an antisymmetric Dzyaloshinskii-Moriya (DM) spin interaction in the CuO planes which gaps the remaining Goldstone mode and leads to a 2<sup>nd</sup> in-plane polarized gap,  $\Delta_{DM}$ , at  $k = 0$  [8]. The same spin-orbit interaction also allows the Raman coupling to one-magnon excitations [9]. Each CuO plane has a weak perpendicular magnetic moment due to the DM interaction but the interplane exchange orients the canted moments antiferromagnetically as shown in Fig 1a. An external magnetic field  $\vec{H} \parallel \hat{c}$  leads to a weak-ferromagnetic (WF) transition [6, 10] depicted in Fig. 1b.

In this Letter we study low energy Brillouin zone center magnetic dynamics in lightly doped  $\text{La}_{2-x}\text{Sr}_x\text{CuO}_4$  as a function of doping, temperature and magnetic field. Two magnetic modes are observed in the AF phase. The one at lower energies is the spin-wave gap induced by the antisymmetric DM interaction and its anisotropic properties in magnetic field can be well explained using a canonical form of the spin Hamiltonian. A new finding is a magnetic field induced mode (FIM) whose dynamics allows us to discover a spin ordered state outside the AF order which is shown to persist in a 9 T field as high as 100 K above the Néel temperature  $T_N$  in  $x = 0.01$ . We propose for the field induced magnetic order a state with a net WF moment in the CuO plane and analyze the FIM in the context of in-plane magnetic anisotropy.

Detwinned single crystals of  $\text{La}_{2-x}\text{Sr}_x\text{CuO}_4$  with  $x = 0 - 0.03$  were grown as described in [4]. The Néel temperatures for the  $x = 0$  and 0.01 crystals studied here are 310 and 215 K respectively in zero field and a decrease of  $T_N$

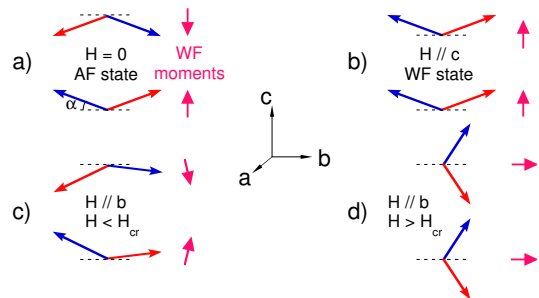


FIG. 1: Cartoon showing spin orientations in two adjacent CuO planes. (a) The 3D AF arrangement in zero applied field and the corresponding orientation of the WF moments in each plane. The canting angle  $\alpha$  from the CuO planes is exaggerated. (b) The WF state. (c) Spin configuration for small fields  $\vec{H} \parallel \hat{b}$ . (d) The proposed spin ordering obtained by further increasing the field  $\vec{H} \parallel \hat{b}$  in (c).

on the average by 1 K/T (for  $x = 0$ ) and almost 4 K/T (for  $x = 0.01$ ) is observed for fields  $\vec{H} \parallel \hat{b}$  axis. We use the notation of the *Bmab* structure for crystallographic axes. We denote by  $(e_{in}e_{out})$  polarization configurations, with  $e_{in/out}$  the direction of the incoming/outgoing photons.  $(RL)$  and  $(RR)$  denote circular polarizations. The crystals were mounted in a continuous flow optical cryostat and the Raman data were taken with incident photon power of a few mW and  $\lambda = 647.1$  nm focused onto  $(ab)$  crystal surfaces. The magnetic field data were taken with the cryostat inserted into the horizontal bore of a superconducting solenoid.

Fig. 2 shows data from  $\text{La}_2\text{CuO}_4$  at 10 K for three directions of the external magnetic field. A sharp resonance is observed in zero field at  $17 \text{ cm}^{-1}$ . This resonance disperses upwards (downwards) for  $\vec{H} \parallel \hat{a}$  ( $\vec{H} \parallel \hat{b}$ ). For  $\vec{H} \parallel \hat{c}$ -axis the mode disperses downwards until  $H_{WF} \approx 6 \text{ T}$  where the transition to the WF state (Fig. 1b) takes place [6, 10]. In the 6 - 7 T range the resonance remains around  $15 \text{ cm}^{-1}$  but decreases in intensity with a concomitant appearance of another feature around  $21 \text{ cm}^{-1}$ . In Fig. 2e-f we show hysteretic loops for the  $21$  and  $15 \text{ cm}^{-1}$  modes intensities, very similar to the behavior of the  $(100)$  and  $(201)$  magnetic Bragg peaks [11], reflecting the dynamics of magnetic domains in the presence of small crystalline imperfections.

The nature of the mode shown in Fig. 2 can be understood by analyzing the spin Hamiltonian [8]

$$\mathcal{H} = \sum_{\langle i,j \rangle} [(J + \alpha)(S_i^x S_j^x + S_i^y S_j^y) + JS_i^z S_j^z + \vec{d}(\vec{S}_i \times \vec{S}_j)] - \vec{H} \sum_i \vec{S}_i \quad (1)$$

where  $J, \alpha, \vec{d}, \vec{H}$  and  $\vec{S}_i$  are the isotropic Heisenberg exchange, the in-plane anisotropy, the DM vector, the external field and the spin on lattice site  $i$ . We calculated the dispersion of the  $k = 0$  spin-wave modes for different magnetic field orientations at  $T = 0$  K by minimizing  $\mathcal{H}$  and linearizing the equations of motion [12]. The inset of Fig. 2d shows the results of this semi-classical calculation for the behavior of the DM gap assuming a full moment on Cu sites,  $\vec{d} \parallel \hat{a}$  and  $\Delta_{DM} = 17 \text{ cm}^{-1}$ . The agreement between the experimental data and the calculation is quantitative allowing us to assign this mode to  $\Delta_{DM}$  and to confirm the validity of the spin-wave approximation. The similar field dispersion for  $\vec{H} \parallel \hat{b}$  versus  $\vec{H} \parallel \hat{c}$  ( $H < H_{WF}$ ) is intriguing because this degeneracy does not follow from the model and it rather suggests rotational symmetry with respect to the  $a$ -axis. The energy of the DM gap is also in agreement with the DM gap value inferred from inelastic neutron scattering (INS) measurements [2, 13]. The softening of the DM gap for  $\vec{H} \parallel \hat{b}$  explains the decrease of  $T_N$  and implies the possibility of a magnetic instability by further increasing the field in this configuration. In principle our data allows also for a

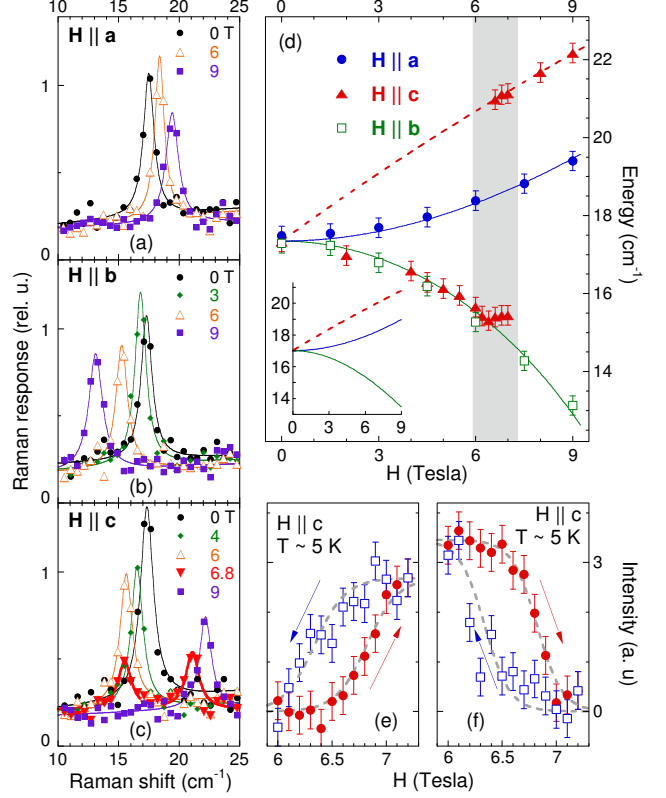


FIG. 2: Panels (a-c) show 10 K ( $RL$ ) polarized Raman spectra of the DM gap in  $\text{La}_2\text{CuO}_4$  with the external field  $\vec{H}$  parallel to the  $a$ ,  $b$  and  $c$ -axes. Solid lines are Lorentzian fits. In (c) the 6.8 T spectrum shows the coexistence of the AF and the WF states. (d) shows the field dependence of  $\Delta_{DM}$  for  $\vec{H} \parallel \hat{a}$  (circles),  $\vec{H} \parallel \hat{b}$  (squares) and  $\vec{H} \parallel \hat{c}$  (triangles). The  $\vec{H} \parallel \hat{c}$  data shows the transition to the WF state depicted in Fig. 1b. The continuous lines are fits with  $\sqrt{\Delta_{DM}^2 + \gamma H^2}$  [ $\Delta_{DM} = 17.35 \pm 0.25 \text{ cm}^{-1}$ ,  $\gamma_{H \parallel a} = 0.96$  and  $\gamma_{H \parallel b} = -1.65 \text{ (cm T)}^{-2}$ ] and the dashed line is a fit to the form  $\sqrt{\Delta_{DM}^2 + \beta H}$  [ $\beta = 22.6 \text{ cm}^{-2}\text{T}^{-1}$ ]. Hysteretic loops of the lower (e) and higher (f) energy DM gaps at the WF transition [shaded area in (d)]. Grey dashed lines in (e-f) are guides for the eye. The inset in (d) shows the results of a semi-classical calculation of the DM gap dispersions as described in the text, see also [12].

quantitative estimation of the magnitude of other higher order spin interactions [3, 14] from magnetic gap renormalization effects. Using the expressions  $\Delta_{DM} = 2.34d$  and  $J = 145 \text{ meV}$  [1, 3] we obtain for  $\text{La}_2\text{CuO}_4$  the value  $d = 0.92 \pm 0.013 \text{ meV}$ .

Doping and temperature dependent properties of the DM gap are shown in Fig. 3. Fig. 3a shows the gap as a function of doping at 10 K. We observe that the DM gap is present only in the AF ordered region of the phase diagram, being absent for  $x \geq 0.02$ . The gap resonance found at  $12.5 \text{ cm}^{-1}$  in  $x = 0.01$  remains sharp but is weaker and has a strongly renormalized energy compared to the undoped case. As a function of temperature, the

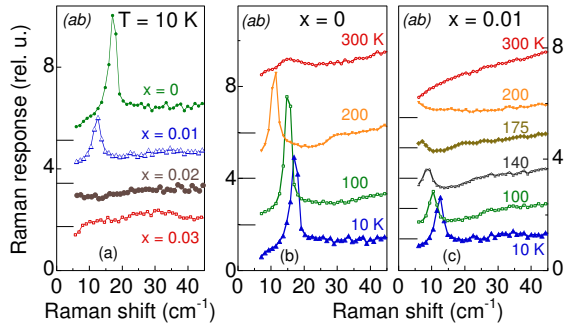


FIG. 3: Doping and temperature dependence of the DM gap in  $\text{La}_{2-x}\text{Sr}_x\text{CuO}_4$  in (ab) polarization for zero applied field. (a) 10 K data for  $x = 0 - 0.03$ . (b-c) Temperature dependent Raman spectra for  $x = 0$  and 0.01. Data are vertically offset.

gap excitation disappears below  $5 \text{ cm}^{-1}$  as we approach  $T_N$  which is indicative of a conventional magnetic soft-mode behavior (Fig. 3b-c). The observed homogeneous renormalization with doping of the DM gap energy at 10 K from  $x = 0$  to  $x = 0.01$  rules out a possible macroscopic phase separation into  $x \approx 0$  and  $x \approx 0.02$  regions suggested in Ref. [15]. Since the DM interaction is induced by lattice orthorhombicity, the decrease of almost 30% at  $T = 10 \text{ K}$  for the gap value between  $x = 0$  and 0.01 is surprising compared to the much smaller decrease in the orthorhombicity and relates it to strong sensitivity to hole doping. Our data suggest that the antisymmetric exchange interaction is strongly competing with frustration and associated spin distortions induced by hole doping [16, 17].

In Fig. 3b there is a broad peak at 300 K around  $15 \text{ cm}^{-1}$  for  $x = 0$  which becomes a kink around  $25 \text{ cm}^{-1}$  at 200 K and disappears with further cooling. The effects of magnetic fields on this excitation for  $\text{La}_2\text{CuO}_4$  are shown in Fig. 4. At 10 K we observe for finite  $\vec{H} \parallel \hat{b}$  a FIM around  $40 \text{ cm}^{-1}$  which is sharp and hardens slightly up to 9 T. At 230 K the FIM is broader and it softens with increasing field gaining spectral weight from the lower energy side. At 300 K we observe qualitatively similar behavior as at 230 K for  $H \leq 6 \text{ T}$  and beyond that value we see the emergence of two independent peaks which harden further with field, see Fig. 4c. Fig. 4b shows the total integrated intensity of the magnetic modes at a given field. The FIMs are not seen for any field direction other than  $\vec{H} \parallel \hat{b}$ .

In  $\text{La}_2\text{CuO}_4$  the FIM dynamics marks two events. The first seems to be a phase transition at 300 K and fields around 6 T. This is indeed the case because we know that the Néel temperature in  $\text{La}_2\text{CuO}_4$  is around 310 K and that the magnetic susceptibility  $\chi_b$  shows  $T_N$  decreasing at a rate of about 1 K/T. Moreover, the narrow widths of the magnetic excitations above 6 T ( $2 \text{ cm}^{-1} \approx 0.25 \text{ meV}$ ) at temperatures more than two orders of magnitude higher (300 K  $\approx 25 \text{ meV}$ ) argue strongly for the collec-

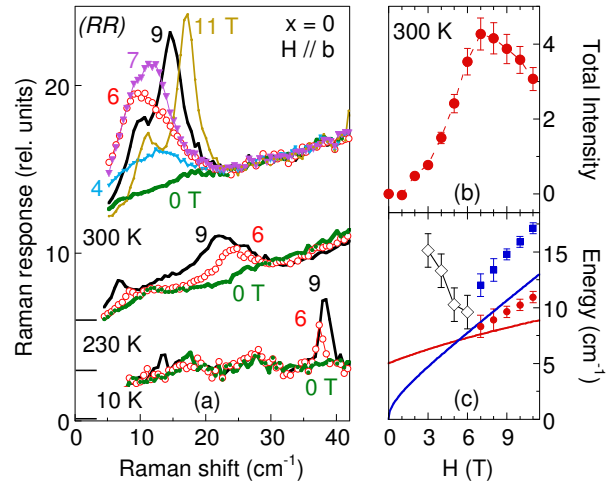


FIG. 4: (a) Magnetic field ( $\vec{H} \parallel \hat{b}$ ) dependence of (RR) polarized Raman spectra in  $\text{La}_2\text{CuO}_4$  at several temperatures. Data are vertically offset. Total integrated intensities obtained by subtracting the 0 T spectrum in (a) from finite field data, panel (b), and the energies, panel (c), of the magnetic modes at 300 K. The lines in (c) are calculated using Eq. (1) with  $\alpha = 0$ , see text.

tive nature of these excitations which correspond to another magnetically ordered state with a well defined gap in the excitation spectrum. The second event, a crossover taking place between 230 and 10 K, is reflected in the opposite dispersion with field and different peak widths at these two temperatures. As for the doping dependence, except for a much weaker intensity (see Fig. 5), we observed the same qualitative behavior in  $x = 0.01$   $\text{La}_{2-x}\text{Sr}_x\text{CuO}_4$ . The FIM is not seen (in fields up to 9 T) at any temperature for  $x \geq 0.02$ .

Fig. 5 shows temperature dependent (RR) polarized spectra in a 9 T field  $\vec{H} \parallel \hat{b}$  for  $x = 0$  and 0.01. The crossover in  $\text{La}_2\text{CuO}_4$  takes place around 150 K, the temperature below which the FIM width narrows. Fig. 5c shows that the intensity of this excitation increases as we approach  $T_N$  and that around 300 K we observe the splitting due to the occurrence of the field induced ordering.

The temperature dependence of the FIM across the Néel boundary can be studied in the  $x = 0.01$  crystal which has a lower  $T_N$ . At 9 T and below 180 K the behavior for  $x = 0.01$  is very similar to that in the undoped crystal showing a softening of the FIM as we warm to  $T_N$ . The 200 K data show that the FIM has, similarly to the 295 K data for  $x = 0$ , a low energy shoulder. We believe that this weak excitation is the softened peak marked by arrows at 250 and 275 K where the data shows the coexistence of two peaks. The lowering in energy can be naturally explained in terms of soft mode behavior above the magnetic transition while below  $T_N$  this mode becomes the DM gap in Fig. 3c. The two peaks above 180 K in  $x = 0.01$   $\text{La}_{2-x}\text{Sr}_x\text{CuO}_4$ , which correspond in

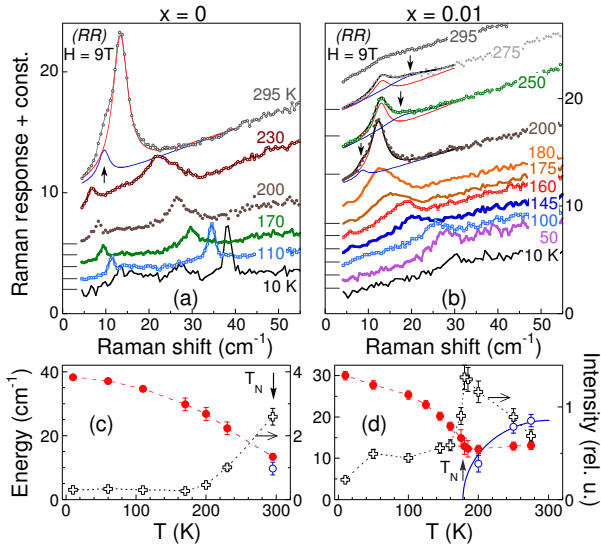


FIG. 5: Temperature dependence of the field induced mode (FIM) in  $\text{La}_{2-x}\text{Sr}_x\text{CuO}_4$  for  $x = 0$  (left) and  $0.01$  (right). (a-b) Data (vertically offset) in (RR) polarization for  $\vec{H} \parallel \hat{b}$  at 9 T. The continuous lines for  $T = 295$  K in (a),  $T = 250$  and  $275$  K in (b) are two-Lorentzian fits to the data. (c-d) Variation with temperature of the FIM energies (circles, left scales) and intensities (crosses, right scales). Empty circles correspond to the arrows in (a-b). The blue line in (d) is a guide for the eye. We also show by arrows the Néel temperatures for  $\vec{H} \parallel \hat{b}$  at 9 T in the two samples.

$\text{La}_2\text{CuO}_4$  to the two features seen in Fig. 4c above 6 T, show that at 9 T the new magnetic order extends up to about 100 K above  $T_N$ . In comparison, the strong feature at 200 K situated at  $12 \text{ cm}^{-1}$  hardens only slightly with increasing temperature, see Fig. 5d. This panel also shows that the intensity of the FIMs is peaked at  $T_N$  which is unexpected in a conventional picture where intensities of long wavelength gap modes scale with the AF order parameter as  $T_N$  is approached from below [13].

A possible explanation for the FIM is its identification to the XY gap. Support for this assignment is the presence of this mode only in  $x = 0$  and  $0.01$   $\text{La}_{2-x}\text{Sr}_x\text{CuO}_4$  as well as the comparison to INS data [2, 13] which estimates  $\Delta_{XY} \approx 40 \text{ cm}^{-1}$  at 10 K. Eq. (1), which described well the DM gap, is also in support because it predicts (at  $T = 0$  K) a shift of about 6% of the XY gap from 0 to 9 T, consistent with the small hardening we observe at 10 K in Fig. 4a. As to the nature of the induced order, we propose a state like the one depicted in Fig. 1d. This is suggested by the magnetic susceptibility data which shows that the moments on Cu sites remain confined in the  $(bc)$  plane above  $T_N$  [4] and also by recent magnetoresistance measurements [6] which are consistent with a gradual rotation of the WF moments. A departure from a two-step transition [18] with an  $a$ -axis spin-flop process occurring between the states shown in Fig. 1c-d is expected because the susceptibility  $\chi_a$  is the smallest

below 300 K for  $x = 0$  and  $0.01$  [4] so the spins cannot partake of the field energy  $-\chi_a H^2/2$ .

This scenario can also explain other observed features. The crossover around 150 K shown in Figs. 4 and 5a may be understood as a departure of the direction of the WF moments from perpendicular to the  $(ab)$  plane to a direction almost parallel to the  $b$ -axis (see Fig. 1) where the XY anisotropy, weaker due to temperature fluctuations, ceases to play a decisive role. Physically, this corresponds to the fact that the conventional out-of-plane XY mode changes its nature as the WF moment rotates away from the  $c$ -axis. Prompted by this idea we calculated (solid lines in Fig. 4c) the spin-wave dispersions using Eq. (1) in the extreme case of  $\alpha = 0$  and a small DM gap which still confines the moments in the  $(bc)$  plane. Although finite temperature effects have to be taken into account, we note that this simple estimation qualitatively reproduces the experimental dispersions. We also comment on the possible relevance of our findings to the switch of orthorhombic axes in magnetic fields [7]. If a state like Fig. 1d is realized (which we show in Fig. 5 to persist to temperatures close to 300 K even for  $x = 0.01$ ) then the magnetic force in an external field is significantly enhanced due to the net in-plane magnetic moment.

The qualitative scenario we propose leaves as open questions the finite Raman coupling to the FIM only for fields  $\vec{H} \parallel \hat{b}$  and also the surprising observation of its temperature dependent spectral weight being peaked at  $T_N$ . However, if we assume that the FIM mode is an excitation other than the XY gap, arising for instance as a result of the 4-sublattice structure, then the common interpretation of the excitation around  $40 \text{ cm}^{-1}$  found in several 2D layered AF's has to be reconsidered.

In summary, we discovered a field induced magnetically ordered phase in detwinned  $x = 0$  and  $0.01$   $\text{La}_{2-x}\text{Sr}_x\text{CuO}_4$ . While the DM gap can be explained within the AF ordered state in the framework of Eq. (1), the behavior of the higher frequency field induced modes both above and below  $T_N$  requires an analysis outside of the traditional interpretation of low energy magnetic dynamics in  $\text{La}_{2-x}\text{Sr}_x\text{CuO}_4$ .

We acknowledge useful discussions with A. N. Lavrov and M. V. Klein.

\* Electronic address: gozar@lucent.com

† Electronic address: girsh@bell-labs.com

- [1] M.A. Kastner *et al.*, Rev. Mod. Phys. **70**, 897 (1998).
- [2] B. Keimer *et al.*, Phys. Rev. B **46**, 14034 (1992).
- [3] R. Coldea *et al.*, Phys. Rev. Lett. **86**, 5377 (2001).
- [4] A.N. Lavrov *et al.*, Phys. Rev. Lett. **87**, 017007 (2001).
- [5] Y. Ando *et al.*, Phys. Rev. Lett. **88**, 137005 (2002).
- [6] Y. Ando, A.N. Lavrov, and S. Komiya, Phys. Rev. Lett. **90**, 247003 (2003).
- [7] A.N. Lavrov, S. Komiya, and Y. Ando, Nature **418**, 385

(2002).

[8] C.J. Peters *et al.*, Phys. Rev. B **37**, 9761 (1988).

[9] P.A. Fleury and R. Loudon, Phys. Rev. **166**, 514 (1968).

[10] T. Thio *et al.*, Phys. Rev. B **38**, 905 (1988).

[11] M.A. Kastner *et al.* Phys. Rev. B **38**, 6636 (1988).

[12] Because Eq. (1) neglects the interplane interaction it cannot be used to account for the region  $\vec{H} \parallel \vec{c}$  ( $H < H_{WF}$ ).

[13] B. Keimer *et al.*, Z. Phys. **91**, 373 (1993).

[14] L. Shekhtman, A. Aharony, and O. Entin-Wohlman, Phys. Rev. B **47**, 174 (1993).

[15] M. Matsuda *et al.*, Phys. Rev. B **65**, 134515 (2002).

[16] A. Aharony *et al.*, Phys. Rev. Lett. **60**, 1330 (1990).

[17] R.J. Gooding *et al.*, Phys. Rev. B **55**, 6360 (1997).

[18] T. Thio *et al.*, Phys. Rev. B **41**, 231 (1990).